

Fracture patterns and their relations to mountain building in a fold-thrust belt: A case study in NW Taiwan

HAO-TSU CHU^{1,5}, JIAN-CHENG LEE^{2,5}, FRANÇOISE BERGERAT^{3,5}, JYR-CHING HU^{4,5}, SHEN-HSIUNG LIANG^{4,5},
CHIA-YU LU^{4,5} and TEH-QUEI LEE^{2,5}

Key-words. – Taiwan, Fold-thrust belt, Orogenesis, Joint pattern.

Abstract. – The main purpose of this study is to analyse striated micro-faults and other types of fractures (including tensile and shear joints, and veins), in order to elucidate their relationships with regional folds and thrusts and regional tectonic stress. We take the fold-thrust belt (i.e., the foothills and the Hsuehshan range) in NW Taiwan as a case study, which is a product of the Plio-Pleistocene arc-continent collision. A total of about 760 and 1700 faults and other fractures, respectively, were collected at 41 sites in the field. We have identified four sets of bed-perpendicular joints in the study area. The observation of joints and bedding at each site indicates that most of the penetrative joint sets developed in the earlier tectonic stage of the pre-folding/pre-tilting event, illustrating the fact that the intersection of joint sets lies along the line perpendicular to the bedding plane. We thus interpret these sets as tectonic fractures under deep-seated tectonic stress. We used the regional fold axes as reference to define the four fracture sets. However, we found that complexity in the study area makes this rather tentative. Principal stress axes σ_1 , σ_2 , σ_3 , were calculated by means of inversion of fault slip data at each site. The ratio Φ that defines the shape of stress ellipsoid is generally small, indicating that the value of the maximum principal stress axis σ_1 is much larger compared to that of σ_2 and σ_3 , which are approximately equal. The paleostress regime was characterized by a combination of thrust and strike-slip tectonic regimes. Based on their geometric relationships with tilted bedding, we found most of striated micro-faults were strongly related to the regional folding and can be categorized as early-, during, and late-folding stages. We characterized two major directions for the compressive event, oriented N110-120°E and N150-160°E respectively, which provide additional evidence to delineate the debates about paleostress changes in the Taiwan mountain building process.

Les réseaux de fractures et leurs relations avec l'orogénèse dans une chaîne plissée : le cas du NW de Taiwan

Mots-clés. – Taiwan, plis, Chevauchements, Orognèse, Réseau de diaclases.

Résumé. – L'objectif principal de cette étude est d'analyser divers types de fractures, incluant plans de failles striés, diaclases et veines, afin d'élucider leurs relations avec les orientations locales et régionales des plis et des contraintes tectoniques. Nous considérons l'exemple de l'orogène NW de Taiwan (foothills et chaîne de Hsuehshan) qui s'est développé lors de la collision arc-continent au Plio-Pléistocène. Dans cette zone, on a mesuré 760 failles et 1700 autres fractures, dans 41 sites. Nous avons identifié quatre ensembles de diaclases perpendiculaires à la stratification. L'observation de celles-ci indique que la plupart ont été développées dans une phase tectonique anté-plissement/basculement, l'intersection des différentes familles de joints se trouvant dans une ligne perpendiculaire à la stratification. Nous avons donc interprété ces diaclases comme des fractures tectoniques créées sous une contrainte tectonique profonde. Nous avons utilisé les axes de pli régionaux comme référence pour définir les quatre ensembles de diaclases. Cependant, la complexité de la zone d'étude rend parfois cette analyse incertaine. Les axes des contraintes principales σ_1 , σ_2 , σ_3 , ont été calculés à partir de l'inversion de données de glissement des failles striées dans chaque site. Le rapport Φ , qui définit la forme de l'ellipsoïde des contraintes, est généralement faible, ce qui indique que la valeur de la contrainte principale maximale σ_1 est beaucoup plus importante que celles de σ_2 et σ_3 , qui sont approximativement égales. Le régime de paléocontraintes est caractérisé par une combinaison de décrochements et de failles inverses/chevauchantes. Sur la base de leurs relations géométriques avec la stratification, nous montrons que la plupart des failles striées sont fortement liées au plissement régional et peuvent être classées comme anté-, syn- et post-plissement. Nous caractérisons deux directions majeures pour la tectonique compressive, N110-120°E et N150-160°E, alimentant ainsi les débats sur les changements de direction des paléocontraintes lors du processus de formation de l'orogène taiwanais.

1. Central Geological Survey, MOEA, Taipei, Taiwan, ROC

2. Institute of Earth Sciences, Academia Sinica, Taipei, Taiwan, ROC. Corresponding author : jcllee@earth.sinica.edu.tw

3. ISTeP, UMR 7193 CNRS-UPMC, Paris, France

4. Department of Geosciences, National Taiwan University, Taiwan, ROC

5. International Laboratory "ADEPT", CNRS-NSC France-Taiwan

Manuscript received on March 31, 2012; accepted on October 19, 2012

INTRODUCTION

Shear fractures and tensile fractures are the most prominent fracture types in the brittle regime of crustal rocks. Amongst fractures *s.l.*, faults accommodate small to large shear strains (e.g., due to different earthquake magnitudes), some other fractures may form under small differential stresses with little or no displacement and have been called joints a long time ago [Hodgson, 1961a, b]. In this paper we consider the term fracture as any tectonic discontinuity, whatever its size, separating a rock mass into two parts [e.g., Gudmundsson, 2011]. Consequently, even if nowadays the term “joint” is preferably used for mode I fractures and because the term “shear fracture” remains indefinite, we prefer to use herein the original terms tensile joints and shear joints for fractures without displacement, which are visible to the naked eye (see discussion in section: Analysis of fracture patterns). As they are often observed coevally with faults, these three types of fractures can provide information about how fractures evolved in response to tectonic emplacement [e.g., Lacombe *et al.*, 2011; Tavani *et al.*, 2011] and their relationship with tectonic stress regime [e.g., Hancock, 1985; Cosgrove and Engelder, 2004]. It is helpful to understand the temporal faults- tensile and shear joints relationships and their chronological relationship with folding in order to better elucidate the structural evolution of rocks under tectonism.

The relevant relationship between fold and fractures pattern has been illustrated in several geological contexts such as platforms (e.g., the Colorado plateau: Bergerat *et al.*, 1991, 1992; Bouroz *et al.*, 1989) and fold-and-thrust belts regions, for example the Jaca thrust-top basin, in Spanish Pyrenees [Turner and Hancock, 1990], the Rattlesnake Mountain anticline [Beaudoin *et al.*, 2012] and the Sheep Mountain anticline [Bellahsen *et al.*, 2006] in the Laramide belt in USA, the Zagros mountains in Iran [Ahmadhadi *et al.*, 2008; Lacombe *et al.*, 2011; Casini *et al.*, 2011], the north Umbria fold belt in Italy [Marshak *et al.*, 1982], the southwestern Basque-Cantabrian belt [Quintà and Tavani, 2012] and the southern Pyrenees [Tavani *et al.*, 2006, 2011] in Spain, and many others. As a few examples, Bellahsen *et al.* [2006] identified five main fracture sets in the Sheep Mountain anticline and were able to reconstruct the chronology of different fracture sets during the growth of the anticlinal fold. Tavani *et al.* [2011] found that the fractures in the Sant Corneli Boixols anticline, including faults as well as tensile and shear joints, not only can develop in the pre-folding stage by reactivating inherited structures but also create new sets in response to the fold growth. Lacombe *et al.* [2011] observed three typical tectonic joint sets in the Zagros simply folded belt and found that two sets had been formed before the folding. One set which is parallel to the fold axis is probably syn-folding, and most of the micro-scale faults, including reverse and strike-slip faults, are either syn-folding or post-folding. One of the aims of this paper is to present the main fracture patterns in the fold-thrust belt of NW Taiwan, in an attempt to provide insights on the characteristics of fracture patterns in brittle regimes and their relationships with regional structures such as folds.

The methods to determine paleotectonic stress regimes and the orientations of related principal axes derived from fault-slip measurements at the outcrop scale have been

successfully developed since about 40 years ago, first in France [e.g., Angelier, 1975, 1979a, b, 1984; Carrey and Brunier, 1974; Armijo and Cisternas, 1978; Etchecopar *et al.*, 1981; for comprehensive reviews and recent progress, see: Célérier *et al.*, 2012; Hippolyte *et al.*, 2012; Lacombe, 2012], and widely applied in many places in the following decade [e.g., Angelier *et al.*, 1986; Barrier, 1985; Barrier *et al.*, 1982; Bergerat, 1985, 1987; Mercier *et al.*, 1976], then everywhere in the world. Field observations together with borehole cores and seismological data showed that faulting with striated planes could occur at a quite large range of different depths, from a few tens of kilometers to shallow crust. Furthermore, it is common to observe multiple phases of tectonic stress regimes in outcrops [Angelier *et al.*, 1990]. As a result, it became a common practice to reconstruct the evolution of tectonic stress regimes in a mountain belt by conducting fault-slip analyses at geological outcrops, such as that in the study area of NW Taiwan [e.g., Angelier *et al.*, 1990; Chu, 1990; Lu *et al.*, 1995; Lee *et al.*, 1997; Mouthereau *et al.*, 1999, 2002; Lacombe *et al.*, 2003; Mouthereau and Lacombe, 2006]. One of the aims of this paper is thus to compile the previous results, some unpublished, to complement the fracture patterns observed and analyzed in this study, and, in particular, to provide constraints on tectonic stress orientations and regimes during mountain building in NW Taiwan.

By contrast, the relationship between tensile and shear joints and tectonic stress and regional folding is more complex and subtle. A wealth of papers on tensile and shear joints/jointing, concerning both their origin and detailed regional description, have been published since about a century ago [for a synthetic review, see Pollard and Aydin, 1988]. Although joints have been recognized a long time ago [Hodgson, 1961a, b] and categorized into different types with their deformation modes [e.g., Hancock, 1985; Engelder and Gross, 1993], determination of tectonic stress orientations from joint sets remains questionable and sometimes problematic, especially because their mechanical significance remains disputable. We acknowledge herein that these fractures can be formed either under tension as tensile features (such as veins, dykes etc.) or by shearing as shear fractures (such as faults) with, in both cases, no displacement visible by naked eyes. In the first case, the planes of joints are always perpendicular to the minimum stress axis σ_3 ; in the second case, they are oblique to the maximum (σ_1) and minimum (σ_3) stresses, and, when conjugate sets of shear fractures develop, the bisector of the acute dihedral angle indicates the direction of σ_1 . Hancock [1986] described a third category that includes hybrid joints with both shear and tensile components. Among the different genetic developments of fracturing, tectonic shear and tensile joints can thus be considered as the two main types that are presumably closely related to deep-seated tectonic stress [Price and Cosgrove, 1990]. During recent decades, some field applications indicated that systematic fracture sets can develop synchronously with a major thrust [e.g., Turner and Hancock, 1990] or coeval with a major regional fold [e.g., Bellahsen *et al.*, 2006; Lacombe *et al.*, 2011; Tavani *et al.*, 2011] and that fractures (i.e., tensile and shear joints) and faults often interact with each other. The temporal relationship between them could be solved based on detailed observations and analyses [Peacock, 2001; Bellahsen *et al.*, 2006; Lacombe *et al.*, 2011].

In this paper we report observations and analyses on brittle features in the fold-thrust belt of NW Taiwan, in which fractures including faults, tensile and shear joints occur under presumably the same stress regimes but could be different if multiple major tectonic events occurred. The chronological analyses of the faults in the study area allow us to categorize them into four groups: pre-, syn-, late-syn-, and post-folding (or -tilting) groups with corresponding orientations of stresses, as the thrust sheets moved from depth to surface. As for the joints, we found that the dominant sets of joints occurred almost exclusively at the earlier stage before the strata were folded or tilted by major thrust systems. Analysis of temporal fault-tensile and shear joints relationships shows that the late stage faulting (syn- and post-fold faulting) caused reactivation of the pre-existing sets of joints developed during the earlier stages. This is possibly the result of the horizontal rotation of regional strata [see for example discussion in Sonnette, 2012] and/or a change in the direction of plate motion, complicating the determination of paleostress orientation that prevailed during development of pre-folding/pre-tilting joint sets.

In what follows, we first present the tectonic and geological background of the Taiwan mountain belt and the fold-thrust belt in NW Taiwan. We then present the methods used in this study, including fracture patterns analysis, fault-slip data analysis, and determine the relative chronology among structures, including regional folds. This is followed by the results on the main fracture sets identified in the four sub-regions of the study area. We then discuss the seeming reactivation of the faults superimposed on the pre-existing joints formed at an earlier stage before and/or during the stacking of thrust sheets in the fold-thrust belt of NW Taiwan, the different responses of development of fractures in the very young Pliocene rocks, and the relationship between the regional tectonics stress and joint sets.

GEOLOGICAL FRAMEWORK

The Taiwan mountain belt and arc-continent collision

The island of Taiwan is the result of an active collision between the Luzon volcanic arc at the western edge of the Philippine Sea plate and the Chinese continental margin, starting since about 5 Ma [Teng, 1992] (fig. 1a). Based on studies on magnetic anomalies on the ocean floor, Seno [1977] stated that the two plates converge in the north-west-southeast direction at a rate of about 70 km/Ma (i.e., 7 cm/yr) in the vicinity of Taiwan. This value is close to a N310°-directed convergent rate of 8.2 cm/yr, derived from recent GPS measurements during the last two decades [Yu *et al.*, 1997; Hsu *et al.*, 2009]. Suppe [1981] later defined the kinematic parameters of oblique plate collision and estimated a SSW propagation rate of collision of 95 km/Ma along the Chinese continental margin.

Combining the age data from the sedimentological and paleontological studies [Chi, 1981; Chang and Chi, 1983], the studies of the fault-slip measurements and the yielded paleostress trajectories in Taiwan [Barrier, 1985; Angelier *et al.*, 1986; Barrier and Angelier, 1986] indicated that the direction of the relative movement of the Philippine Sea plate changed counterclockwise about 50° from NNW to NW during the Neogene. According to these studies, the

beginning of the collision is related to such changes in the direction of plate movement. However, Lacombe *et al.* [2003] combined the above previous data with newly acquired fault kinematic data, and incorporating additional evidence of relative chronology between the different stages of tectonic compression, claimed that the Foothills in NW Taiwan had experienced two major tectonic stages: N120° compression first, followed by N150° compression in northern NW Taiwan and continuing N120° compression in southern NW Taiwan, without significant regional block rotation. Consequently, this paper also intends to shed insights on this controversy by providing more evidence. Note however Lacombe *et al.* [2003] additionally claimed that “this succession does not require two major tectonic events which are unlikely to have occurred during the short time span considered, and may simply result from a local evolution through time of the regional stress regime in response to the complex kinematics of the collision in NW Taiwan”.

The foothills and the Hsuehshan Range in NW Taiwan

Starting from 6 to 4 Ma ago, plate collision and associated mountain building have been going on in Taiwan. Arc-continent collision is mainly responsible for the emergence of the Central Range, with impressive topography at nearly 4000 meters high. The 400 km long, 100-to-150 km wide Taiwan mountain belt is composed of deformed rocks of the Pre-Cenozoic metamorphic basement and the overlying thick Cenozoic sedimentary sequences of the Chinese continental margin. The moderately deformed sedimentary formations of the fold-thrust belt, including the foothills and Hsuehshan Range (the western Slate belt) to the west of the Central Range (fig. 1) with numerous outcrops, provide a good opportunity to study faults and fractures in terms of relationships among tectonic stress, regional folding/thrusting and fracturing processes. Consequently, our study area is confined to the fold-thrust belt in NW Taiwan (fig. 1b).

The age of the rocks in the study area ranges from Eo-Oligocene pre-orogeny shallow marine deposits (Hsitzun Fm) to Plio-Pleistocene syn-orogeny terrestrial foreland deposits (Cholan Fm) (fig. 1b; table I). The sedimentary sequences of the foothills are mainly composed of shallow marine to shelf clastic sediments including sandstones, siltstones, mudstones, calcareous sandstones, and shales. Calcareous sediments are rare. Coal-bearing formations are mainly distributed in the Miocene formations in the northern part of the study area. The foothills is further subdivided into outer foothills and inner foothills according to their intensity of deformation and proximity to the foreland [Ho, 1982]; however, this separation is somewhat subtle and is therefore not commonly adopted.

To the east of the foothills is the Hsuehshan Range (fig. 1b). It is mainly composed of abundant thick quartz-rich sediments. Shale and sandstone of the Hsuehshan Range are slightly metamorphosed under zeolite facies to prehnite-pumpeleite facies metamorphism [Chen *et al.*, 1983]. Generally speaking, the main deformation style of Hsuehshan Range is similar to that of the inner foothills, but with more intense and denser deformation structures. The boundary between the foothills and the Hsuehshan Range is the west-vergent Chuchih-Shuichangliu thrust fault system (fig. 1b).

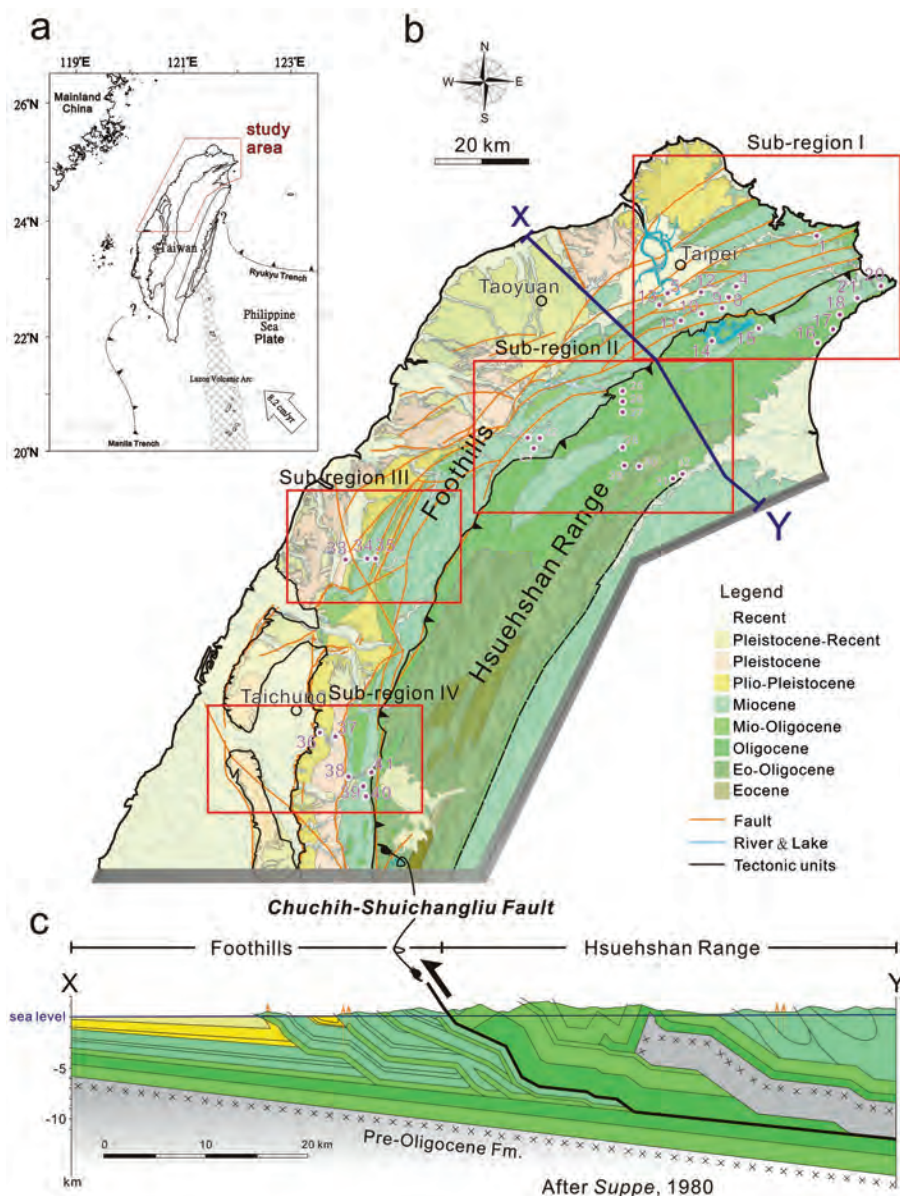


FIG. 1. – (a) Geodynamical context of the Taiwan collision. Subduction zone as thick lines with barbs on the overriding side. (b) Detailed geology and site locations of the study area in fold-and-thrust belt of northern Taiwan, including foothills (III) showing the outer fold-thrust zone and the Hsuehshan range (II) showing the inner fold-thrust zone [after Ho, 1982]. The boundary between the foothills and the Hsuehshan Range is represented by the major faults of the Chuchih-Shuichangliu fault system [after Ho, 1982]. Red rectangles marks the sub-regions I, II, III, and IV. (c) General geological cross-section across the northern Taiwan, showing the study area is characterized by thrust sheets stacked along several reverse faults [after Suppe, 1980].

The deformation in the foothills is generally characterized by a sequence of sub-parallel imbricate thrusts with less intense folding between thrust sheets (see also cross section in fig. 1c). On the other hand, although the deformation in the Hsuehshan range is also characterized by sub-parallel thrusts, the folding structures become more dominant (fig. 1b and 1c) and their wavelengths vary probably as a function of grain size and thickness of the sedimentary layers (the smaller the grain size and the thicker the massive sandstone layer, the longer the wavelengths). It is worth noting that some of the major thrusts in the fold-thrust belt are also controlled by regional salient and recess structures [Lacombe *et al.*, 2003], which reactivated the pre-orogenic normal faults in a tectonic inversion fashion [Yang *et al.*, 1996; Mouthereau *et al.*, 1999; Lacombe *et al.*, 2003], in

particular the E-W trending faults along the southern edge of the Kuanyin high in the north of the study area and the N-S trending faults along the northern edge of the Peikang high in the south.

METHODS

In this study, we present data from 41 field sites (20 sites in foothills and 21 sites in Hsuehshan Range) in NW Taiwan. About 2,500 fractures (including faults, tensile and shear joints, veins) and bedding planes were measured. All sites are tabulated in table I and shown in figure 1. Most of the joints were measured within sandstones, siltstones and shales.

TABLE I. – General information of studied sites, including geographic coordinates, stratigraphy, age of rock formation and type of structures analyzed. Site location: see in figure 2, 5, 6 and 7. JN: bedding; J: joint; JX: tension vein; FI: suspected reverse fault without striation; N: normal fault; D: right-lateral strike-slip fault; S: left-lateral strike-slip fault; I: reverse fault (C: certain; P: probable; S: suspected); MC: fracture cleavage.

SITE NO	LATITUDE	LONGITUDE	STRATIGRAPHY	AGE	TYPE OF STRUCTURE	Sub-region
1	25°06.5'	121°49.5'	TALIAO F	MIO (L)	JJN	I
4	25°00.5'	121°39'	TALIAO F	MIO (L)	JJN	I
5 5A	25°00'	121°30'	TALIAO F	MIO (L)	J CI JN	I
5B	25°00'	121°30'	MUSHAN	MIO(L)	J CI JN PD PI	I
8	25°01.5'	121°40'	SHITI	MIO (L)	JJN CS	I
9	25°01.5'	121°39.5'	SHITI	MIO (L)	JJN CS	I
10	24°57'	121°36.5'	NANKANG	MIO (M)	J	I
11	24°57'	121°36'	KUANYIN	MIO (L)	JJN	I
12	25°00.5'	121°33'	SHITI	MIO(L)	JJN CS	I
13	24°59'	121°29'	JUIFANG G.	MIO (M)	JJN CD	I
14	24°55.3'	121°37'	SZELENG	OLIG(L)	JJN CS CD CI	I
14A	24°54'	121°35'	SZELENG F	OLIG	JJN CS CD CI	I
15	24°55.5'	121°42'	MUSHAN	MIO (L)	JJN CI	I
15	24°55.5'	121°55.5'	MUSHAN F	MIO (L)	JJN CI CS CD	I
16	24°53'	121°50'	TSUKU	OLIG	JJN JX	I
17	24°55'	121°52.4'	TSUKU	OLIG	J CD	I
18	24°53.1'	121°50.2'	KANKOU	OLIG	JJN CD CI JX MC	I
20	25°00.5'	121°59.5'	TATUNGSHAN	OLIG	J	I
21	24°55.1'	121°52.5'	KANKOU	OLIG	JJN CD	I
22	24°42'	121°13'	PEILIAO F	MIO (L)	J CD JN CS	II
23	24°42'	121°12.5'	PEILIAO F	MIO (L)	JN J CD CI CS	II
24 24A 24C	24°42.5'	121°12'	PEILIAO F	MIO (L)	JJN	II
25	24°48'	121°22'	MUSHAN F	MIO (L)	JJN CI	II
26	24°47.5'	121°22'	MUSHAN F	MIO (L)	JJN CS CD CI	II
27	24°47'	121°22'	MUSHAN F	MIO (L)	CS CD J PD	II
28 28B	24°41'	121°22°	MUSHAN F	MIO (L)	JJN CS CD CI	II
29	24°39'	121°22'	SZELENG F	OLIG	JJN CD CS	II
29B	24°39'	121°23'	SZELENG F	OLIG	JJN CD CS	II
30	24°39'	121°28'	SZELENG F	OLIG	JJN CD CS CJX	II
31	24°37'	121°33'	SZELENG F	OLIG	JJN JX	II
32	24°37'	121°33.5'	SZELENG F	OLIG	JJN CD CN CI	II
33	24°08'	120°49.5'	KUEICHULIN F	PLI-PLI	JJN PS	III
34	24°28'	120°55.5'	PEILIAO F	MIO (L)	CI CS CD CN	III
35	24°28'	120°51'	PEILIAO F	MIO (L)	CI CS CN CD J	III
36	24°07'	120°45'	CHOLAN F	PLI-PLI	JJN	IV
37	24°06.5'	120°47'	CHOLAN F	PLE-PLI	JJN	IV
38	24°02'	120°48'	KUEICHULIN F	PLE-PLI	JJN	IV
39	23°59.5'	121°51'	PEILIAO F	PLE-MIO	JX CI CN J CN CS CD	IV
40	24°00.5'	120°50.5'	PEILIAO F	MIO (L)	CN CI JN CS	IV
41	24°03'	120°51.5'	TALIAO F	MIO (L)	J CI CS CD PS	IV

Analysis of fracture patterns

The most predominant fracture types consist of tensile and shear joints, and veins. As defined above, the joint surfaces exhibit no displacement under naked eyes, which certainly handicap further kinematic analysis in terms of principal stress orientations. However, surveying other structural features with good kinematic indicator, such as mineralized veins and stylolitic peaks in association with joints might overcome this difficulty to some extent. Regional fold axis and/or an independently derived stress pattern, such as that from fault-slip data, can facilitate the study on the deformation mode of joint sets if analysis of all these types of structures (i.e., regional folds, faults and joints) is carried out at the same sites. Furthermore, detailed observations on the pavement of fractures, such as spacing, continuity, and accompanying minor deformation structures, also help to define the deformation modes of fractures. For instance, the occurrence of horsetail is a good indicator for defining a set of shear fractures. We also used indicators such as plumose structures to define fractures as tensile joints in the field. We found several sites with good exposures of co-existing features. They provide an opportunity to investigate the

relationship between the genesis of tensile and shear joints, faults, regional folding/tilting and associated stress pattern. Favorable conditions for deciphering the mechanical significance of sets of joints are unfortunately not always found for each site, which reveal the complexity of the fracturing in the fold-thrust belt of NW Taiwan. In the following we first describe our methods of analyzing sets of tensile and shear joints.

At each site, we pay attention to the quality of the outcrop, and to the coherence and abundance of fracture set population. A fracture set is generally defined by a narrow spread in the orientation of its members, including strike and dip. The representative sets of joints (tensile or shear joints) were determined statically by clustering of their poles in stereonet. We used computer program OSXStereonet, developed by Cardozo and Allmendinger to conduct and plot the stereonets of fracture patterns at each site. We also used the abutting relationships between fracture sets, when statistically valid, to differentiate the relative chronology among the different sets. Special care was taken for the 12 sites with abundant populations of fractures (both joints and faults) in terms of their geometric and superimposed relationships. Measurements of bedding, en-echelon quartz veins, and pressure solution cleavage, which are also essential, were conducted in the field. All the measurements of brittle features are plotted using Schmidt's stereographic projection. Typically, the representative fracture sets can be obtained by contour calculations of Pi-diagram in Schmidt's stereonet projection. To better determine their chronological relationship with regional folding or tilting, we plotted the average bedding plane with representative fracture sets in the same stereonet at each site. In practice, we found that most of the fracture sets are nearly perpendicular to the bedding plane, implying that they mostly occurred before folding/tilting, although some would possibly be fold-related tensile joints developed during folding. We have aware that tensile joints perpendicular to fold axis can develop at any time during folding. Furthermore, in regions of large deformation of fold-and-thrust belt, the assumption of vertical principal stress must be considered with care [Célérier *et al.*, 2012; Hippolyte *et al.*, 2012; Lacombe, 2012].

Regarding the geometric relation between regional folds and fracture sets, we found there is often a fracture set parallel to the regional fold axis at the observation site, which has long been observed [e.g., Parker, 1942; Bergbauer and Pollard, 2004] and was interpreted as being related to the growth or flexure of fold (i.e., presumably a tensile joint set). Hence it provides an additional criterion to differentiate the deformation modes of fracture sets. We then compared the orientations of representative fracture sets with (i) the compressive stress directions indicated by regional and local fold axes and (ii) the direction of the maximum principal stress axis derived from fault-slip analysis at the same site.

Paleostress and fault-slip data analysis

As mentioned above, striated micro-faults are also common in the brittle deformation of the fold-thrust belt of NW Taiwan, in addition to tensile and shear joints. In this study, we adopted the methods developed by Angelier [1979b, 1984, 1990] to determine the principal stress axes from the fault-slip data sets. Fault populations were measured in the field

outcrops and then analysed using the completed methods of P and T dihedral [Angelier and Mechler, 1977] and stress tensor determinations [Angelier, 1984]. For each population we determined the orientations of the three principal stress axes ($\sigma_1 \geq \sigma_2 \geq \sigma_3$) and the ratio $\phi = (\sigma_2 - \sigma_3) / (\sigma_1 - \sigma_3)$. We adopted the convention that compressive stress is positive and tensile stress is negative.

Analysis of chronology of fractures and their relations with regional folding or tilting

Analysis of the chronological development of fractures (including faults) with respect to regional folding (or tilting) allows their categorization them into four stages: pre-, syn-, late-syn, and post-folding (or -tilting). As mentioned above, we found that most of the main fracture sets are perpendicular to the bedding plane. This strongly indicates a pre-folding (or pre-tilting) deformation stage for fracturing, although a few fracture sets could also possibly be fold-related tensile joints that occurred during folding. Further, the tensile joint sets, which are found to be parallel to the regional fold axis, might be syn-folding. As for the chronological relationship between faulting and folding/tilting, we used a few geometrical criteria to determine the chronology between the folds and the principal stress axes derived from faults in the study area. First, we plot the attitude of bedding together with the yielded orientation of the principal stress axes deduced from fault-slip data at each site. In

cases where one principal stress axis is found to be perpendicular to the bedding, we consider the faulting to belong to pre-folding. Then, we assigned the faults to have formed before folding if the folds and faults had been apparently under different compressive stresses and the faults to have formed as syn-folding if they appear under the same compressive stress. On the other hand, in the cases that no principal stress axis is orthogonal to bedding plane but one is close to vertical instead, we considered the faults to have formed during the late stage of folding if they were under the same compressive stress, and to have formed later than folding if they developed under different compressive stresses, respectively.

It is worth noting that the determination of the maximum principal stress axis σ_1 usually is better defined than σ_2 and σ_3 . In general, most site analyses show that one of the computed σ_2 or σ_3 axes is close to the vertical or sub-vertical direction (both before and after back-tilting), indicating that the thrust or strike-slip tectonic regimes tend to dominate. We interpret the steep plunges of the σ_1 axis at several sites together with a steep plunge of bedding, such as at sites 14B, 34, and 39, to be due to a post-faulting tilt. Therefore, these faulting events are considered to have occurred during pre-folding (or pre-tilting) or early stage of syn-folding (or syn-tilting), i.e., with σ_1 sub-horizontal and sub-parallel to bedding (i.e., layer-parallel shortening). Abutting or crosscutting patterns can help to decipher the

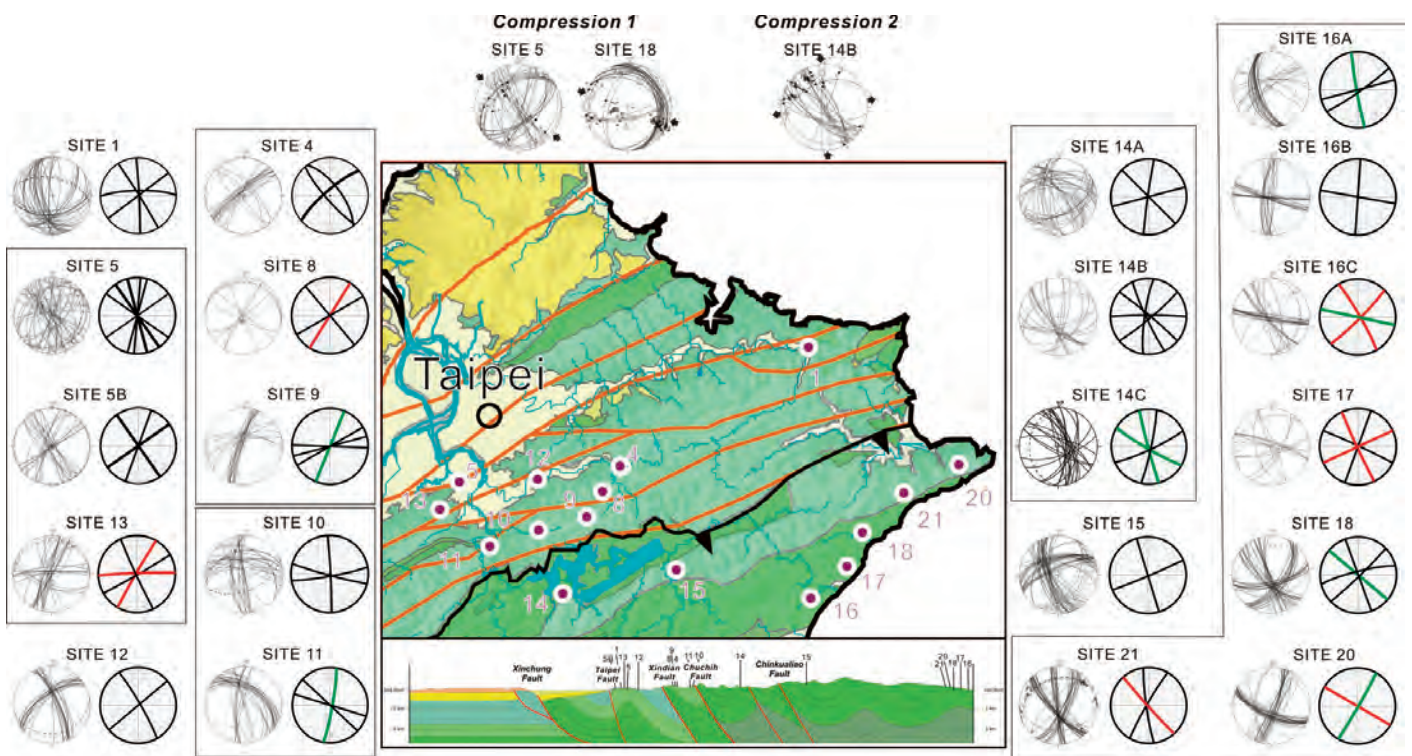


FIG. 2. – Analysis of fractures sets in sub-region I of the studied area (Taipei-Ilan area), the northernmost fold-thrust belt of NW Taiwan. Cross section (across the middle of the sub-region I) shows three to five major thrusts trending N060°-N045° occurred in the Hsuehshan Range. The colors code for different geological rock units are the same as those in figure 1. Examples of results of paleostress analysis and the associated fault-slip measurements are shown in the upper figure. Joints with original data (left) and back-tilted representative sets (right) at each site in the sub-region, are shown. Schmidt’s projection with lower hemisphere is employed. Bedding planes shown as dashed-line great circles. Fault and joint planes shown as thin great circles, with slickenside lineations as dots and arrows indicating the sense of motion (inward direction for reverse slip). Computed stress axes shown as stars with five branches (σ_1), four branches (σ_2), and three branches (σ_3). Method of calculation of stress tensor: Angelier [1984]. In the stereonets of the representative joint sets, heavy lines indicate predominant fracture sets, the tensile joints are in green, the shear joints in red and the undefined joints in black.

chronological relationships between the different fracture sets. However we have to keep in mind that such relationships are not obvious and that only a significant number of data can provide a reliable chronology. For this reason we used the observations of pavements only as a supplement or confirmation of other criteria.

DESCRIPTIONS AND ANALYSES OF MAIN FRACTURE PATTERNS

Hereafter we describe the characteristics of the main fracture patterns analyzed in this paper. We separate the fold-thrust belt of NW Taiwan into four sub-regions (fig. 1b), from north to south: Sub-region I, the Taipei area; Sub-region II, the Taoyuan-Hsinchu-Paling area; Sub-region III, the Miaoli area; Sub-region IV, the Taichung-Puli area.

Sub-region I

The Sub-region I of the Taipei-Ilan area represents the northernmost fold-thrust belt of NW Taiwan (fig. 2). Three to five major thrusts with their associated folds trending N060°-N045° occurred in the foothills and two to three major thrusts trending N060°-N050° occurred in the Hsuehshan Range. In sub-region I, we present the results of fracture analyses at four locations with 10 sites in Foothills and three locations with 7 sites in the Hsuehshan range.

The first location (sites 5, 5B, 13) is close to the Taipei fault in an anticlinal fold of the hanging wall (fig. 2) within the early Miocene Mushan Fm, massive quartzose sandstone with occasional intercalation of shale beds. We found 3-4 bed-perpendicular fracture sets at these three sites. Lacking field evidence, we are not able to identify the fractures at these three sites as tensile joints. On the other hand, we determined two sets of shear fractures as indicated by “Riedel shear” on the fracture planes (see stereonets of site 13 in fig. 2). The J4 set, which we defined as the fracture set with strike parallel to the local fold axis at the sites, can be observed at each site with an orientation of N045° to N060°. Although the fold-parallel fracture is often considered as tensile joint related to folding, however, we did not find field evidence of tensile or opening feature. As a result, the deformation mode of J4 remains inconclusive at the location. The J1 set, which we defined as the fracture sets perpendicular to the local fold axis, is predominant at sites 5 and 5B and less dominant at site 13, showing an orientation of N130° to N160°. As the J4 set, we did not observe good evidence to support the J1 as the tensile joint set, although the compression-parallel tensile joints are rather common in the mountain belt [e.g., Lacombe *et al.*, 2011]. In addition to J1 and J4 sets, we identified two other fracture sets, which are seemingly a conjugate set of shear fractures. The J2 set is predominant at site 13, showing an orientation of N010° to N030°. The J3 set is also dominant at site 13 but somewhat obscure at site 5 and absent at site 5B, showing an orientation of N080° to N120°. At site 13, the J2 set shows a sinistral sense revealed by Riedel shear fractures and the J3 set shows a dextral sense. It appears that all these four bed-perpendicular fracture sets developed prior to the anticlinal fold associated with the Taipei fault, although the evidence of chronological relationships among the fracture sets is not clearly shown at the outcrops.

As for the micro-scale striated faults, we found a set of conjugate strike-slip faults at site 5. The right-lateral slip planes seemingly reactivated the pre-existing fracture, J3 set and the left-lateral shears slipped along the J1 set. The geometric relation of oblique pitch and bedding plane indicates that the strike-slip faulting occurred at the early-folding stage with a N130° compression. We also found conjugate reverse faults at site 5B. The paleostress analysis from these reverse faults shows two episodes of compression: first along N115° and second along N150°. Considering one set of the reverse faults slipped along the bedding planes, we conclude that two episodes occurred during folding, which favors the bedding-parallel slip.

The second location (sites 4, 8 and 9) is located within a gentle anticline, which trends N075°-080°, in the hanging wall of the Xindian fault. The outcrops were observed in the middle Miocene Shiti Fm of shallow marine sandstone and shale intercalation. We observed four bed-perpendicular fracture sets of J1, J2, J3, and J4 at this location. However, these fractures were generally much less developed compared to that from the first location. The predominant fracture sets are J1 (orientation of N005°-010°, i.e., perpendicular to regional fold axis) and J2 (orientation of N030°-N050°). The J4 (orientation of N050°-N065°, i.e., parallel to regional fold axis) and J3 (about N140°) are less marked. At two sites (4 and 8), the J2 and J4 sets are somewhat overlapped. In this case, the distinction between the two becomes difficult. However, we define J2 as a set of shear joints based on its field evidence at site 8. The J1 set was observed only at site 9 and was identified as a tensile joint set with plumose structure. The J3 set was also observed at two sites (4 and

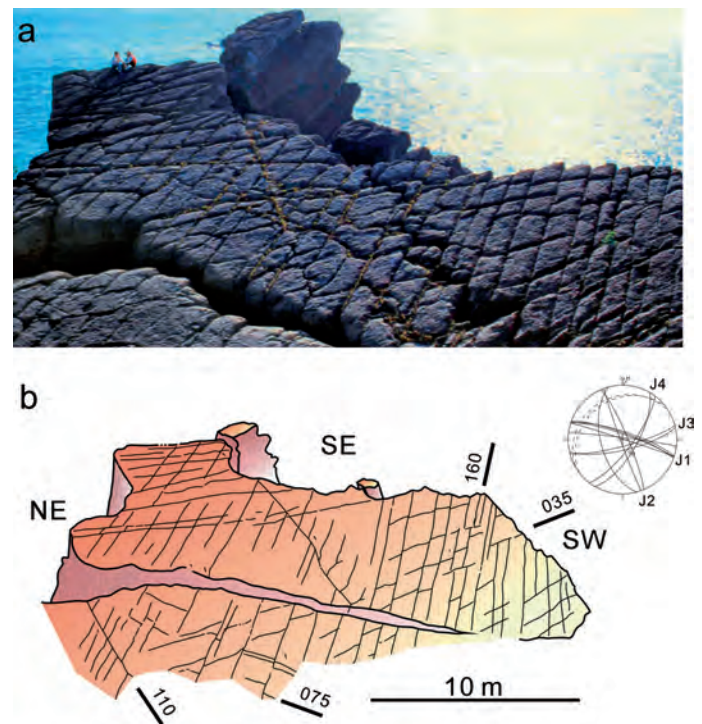


FIG. 3. – Example of the main joint sets. a: photograph of field observation at site 17 (location see figure 2) of the Peikuan area. b: field sketch of co-existence of four different joint sets J4: N035°, J3: N075°, J2: N160°, J1: N110°. A stereonet of the measured fractures at the site is also given. The field observations illustrate some abutting and cross-cutting relationships between the fracture sets (see details in the text).

8) but without solid evidence to reveal its deformation mode. No striated fault was observed so paleostress analysis could not be carried out at this location.

The third location with two sites (10 and 11) is located at the foothills in the footwall of the Chuchih fault, within the middle Miocene Nankang Fm – calcareous massive sandstone. At each site, we could find 2-3 major bed-perpendicular fracture sets. J1 set with orientations of N175° to N195° were observed at both sites, showing plumose tensile joint feature. The J3 and J4 sets are somewhat overlapped with orientations of N085° to N140°. As a result, the identification becomes more difficult and challenging. No striated fault has been observed at the two sites.

The fourth location (sites 16-21) is located in a gentle anticline at the eastern edge of the Hsuehshan Range along the coastline north of Ilan plain (fig. 2). The rocks in this location are the late Miocene to early Oligocene Makang and Tsuku Fms – slightly metamorphosed argillite to sandstone and their intercalation. Fractures such as tensile and shear joints, veins, and faults were mostly measured in massive sandstone layers. On the other hand, pencil cleavages and pressure solution cleavages were measured in fine-grained argillites. We could often find 3-4 predominant sets of bed-perpendicular fractures at each site. Combining the fractures sets at 7 sites including 2 sub-sites, it appeared that the orientations of fractures sets are quite complex and are difficult to categorize into systematic fractures sets according to the orientation relation with the regional fold

axis. This might also be due to possible local block rotations at outcrop scale at this location [e.g., Lu *et al.*, 1995]. Nevertheless, we tried to summarize the fracture sets following the same manners as at previous locations. The J4 fracture set, which is a fold-axis-parallel joint set, was observed at several sites (sites 16, 17, 18) although it is usually less marked, with an orientation of N070° to N090° and sometimes filled with calcite or quartz veins, implying a later opening. The J1 joint set was observed in almost all sites, showing an orientation of N110° to N190°. At sites 18 and 20, we can observe J1 joint set showing plumose tensile structures (fig. 4) The J2 joint set was observed at sites 16C, 17 and 21, showing an orientation of N160° to N045°. The J3 joint set was observed at sites 16B, 16C, 17, 18, 20 and 21 in an orientation of N075° to N140°. An outcrop at site 17 shows abutting and cross-cutting relationships among fracture sets (fig. 3), allowing to obtain a chronological order: J1 joint set (N110°), the longest and rectilinear, was the earliest set, followed by J4 (probably tensile joint, N035°) and J2 (shear joint, N160°), which were almost coeval, and the last one was J3 (shear joint, N075°), the shortest and irregular. All the four bed-perpendicular fracture sets are considered to have formed prior to regional folding. As for striated faults, conjugate sets of reverse faults were commonly observed at each site (fig. 4) with a set of bedding-parallel slip surfaces, implying that they occurred at syn- or late-folding stage. The reverse faults indicate a N115°-130° compression (fig. 2, stereonet in Compression 1).

There are two other sites in the Hsuehshan Range: sites 14 and 15 (fig. 2). Site 14 is located in an anticline in the hanging wall of the Chuchih fault, within the late Oligocene Tsuku Fm. We found 3-4 well-developed bed-perpendicular sets at each three sub-site across the anticlinal fold. The J1 joint set, which is perpendicular to fold axis, is orientated N125° to N160°, showing predominant fractures with a rather wide spectrum of orientations. J2 fracture set orientates N195°, and J4 fractures is orientated N060° to N080°. Because of the exhibited consistency in three sub-sites across the anticlinal fold (i.e., sites 14A, 14B and 14C), we tend to interpret that the three bed-perpendicular fracture sets all occurred prior to the folding. As for striated micro-faults, we observed strike-slip and reverse faults. The strike-slip fault generally used the above fracture sets as slip planes. Their geometric relation with bedding indicates that the strike-slip faulting were both syn-folding (or early folding) and post-folding (or late folding) with a N125° and a N150° compression, respectively. Reverse faults is characterized by bedding-parallel slip with a quite large variation in compression, which is consistent with a possible scenario of two episodic compressive events during folding that can be derived from the strike-slip faults.

Site 15 is located at a synclinal in the middle of the Hsuehshan range, within the early Miocene Makang Fm. We observed two predominant fracture sets, which are perpendicular to bedding: J1 and J4 sets. The J1 fracture set shows a scattered spectrum of orientation of N135° to N180°. The J4 set shows an orientation of N070° to N090°, with quartz veins filling. We tend to interpret these two sets as having formed prior to regional folding. However, a large spectrum also suggests that some sub-parallel fractures might develop during the folding, as proposed by Bergbauer and Pollard [2004]. As for the striated micro-faults, we found strike-slip faults and reverse faults. The strike-slip

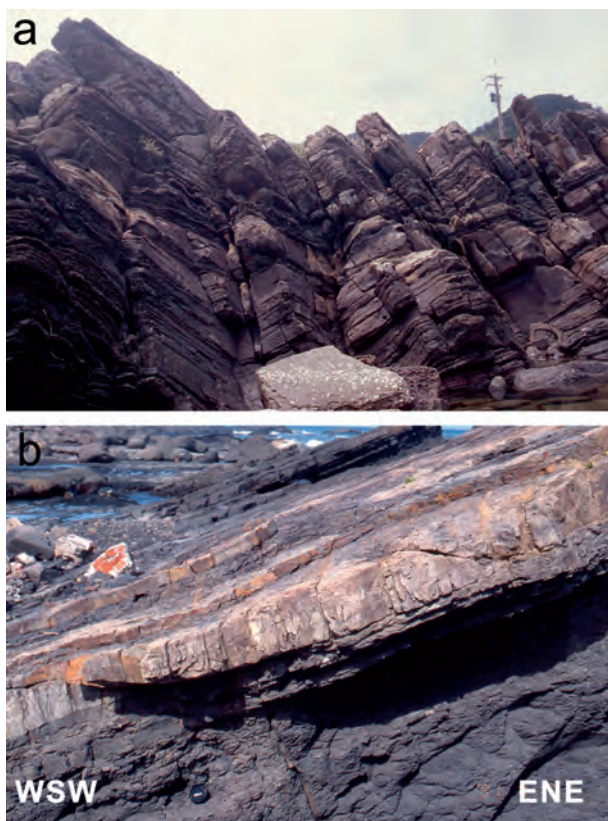


FIG. 4. – Examples of fractures in field outcrops. a: photograph of joints (J1, high angle with strike approximately N-S) with plumose structure as defined as tensile joints at the site 18. b: photograph of micro-striated reverse faults (strike approximately N160° with 10-20° dip towards SW) observed and measured along massive sandstone beds at the site 16.

faults appear to reactivate the pre-existing J1 fracture set as their slip planes. The reverse faults show a conjugate set in which one of them corresponds to bedding-parallel slip surfaces, implying they were syn-folding. The strike-slip faults and reverse faults reveal two episodes with a N130° compression followed by a N180° compression.

Sub-region II

In the Taoyuan-Paling area of sub-region II, we present one location in the foothills (3 sites) and 4 locations in the Hsuehshan range (8 sites) (fig. 5). The sites 22-24 are located in a syncline of the footwall of the Chuchih fault,

which separates the foothills to the west and the Hsuehshan range to the east. We observed 3-4 sets of bed-perpendicular fracture sets at these three sites. J1, J4 and J2 are the most predominant joint sets with orientations of N100° to N175°, N040° to N050° and N000° to N015°, respectively. J1 set, which we defined as the joint set sub-perpendicular to the regional fold axis, reveals a spectrum of a quite a large variation. At site 23, J1 set shows evidence as shear joints. J3 set was observed at sites 24A and 24C, with an orientation of N090° to N105°. We tend to interpret that the four bed-perpendicular joint sets at these three sites all occurred prior to folding. As for striated micro-faults, we found that strike-slip faults occurred mostly along the J1 set as early- or syn-folding

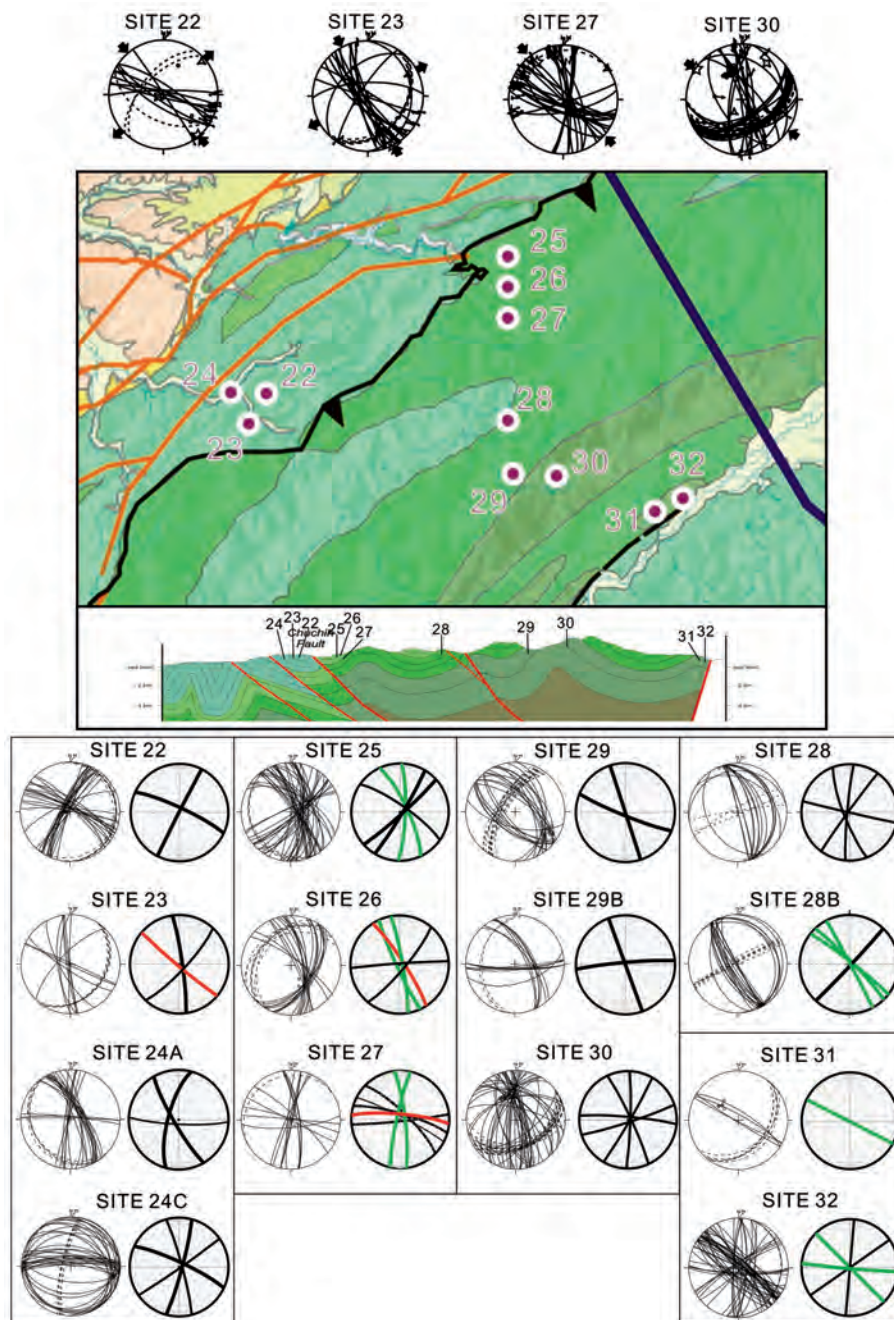


FIG. 5. – Analysis of fracture sets in the Taoyuan-Paling area of sub-region II. We present one location (3 sites) in the foothills and 4 locations (10 sites) in the Hsuehshan Range. Symbols and colors used for fault-slip and joint sets diagrams are the same as in figure 2. The geological profile crosses approximately in the middle of the sub-region. The colors code for the geological rock units is the same as in figure 1.

deformation fractures under a N140°-145° compression. We also observed a conjugate set of reverse faults with a set as bedding parallel slip surfaces, suggesting a syn- or late-folding deformation structures. The reverse faults also show a N145° compression, which are sub-perpendicular to the trend of the regional folds and thrusts, and hence corresponds to a major regional compressional event.

The sites 25-27 are located at a syncline in the hanging wall of the Chuchih fault within the late Oligocene Makang Fm. We observed four bed-perpendicular joint sets at these three sites. J1 set, which was observed at all three sites, is a tensile joint set with an orientation of N150°-175°. The orientation of the J2 joint set is close to J1 set, of about N180°-190°, which makes it difficult to distinguish between the two sets. The spectrum of the tensile joints J1-J2 and the

fracture set J4 (oriented N030°-045°) appear to be the predominant joint sets at sites 25 and 26. However the J4 joints are almost totally absent at site 27, which is characterized by two orthogonal joint sets (J1-J2 spectrum and J3 shear fracture). Striated micro-faults, such as strike-slip and reverse faults are abundant at the three sites. In most of the preceding sites, the strike-slip faults principally reactivated the bed-perpendicular fracture sets as the slip planes. They also showed two episodes: the first one occurred at the very early stage of folding in a N100° compression and the second one occurred at the post-folding stage associated with a N160°-170° compression. Most reverse faults correspond to bedding-parallel slip surfaces. These observations demonstrate the occurrence of two compressional events: an early N115° compression and a later N180° compression.

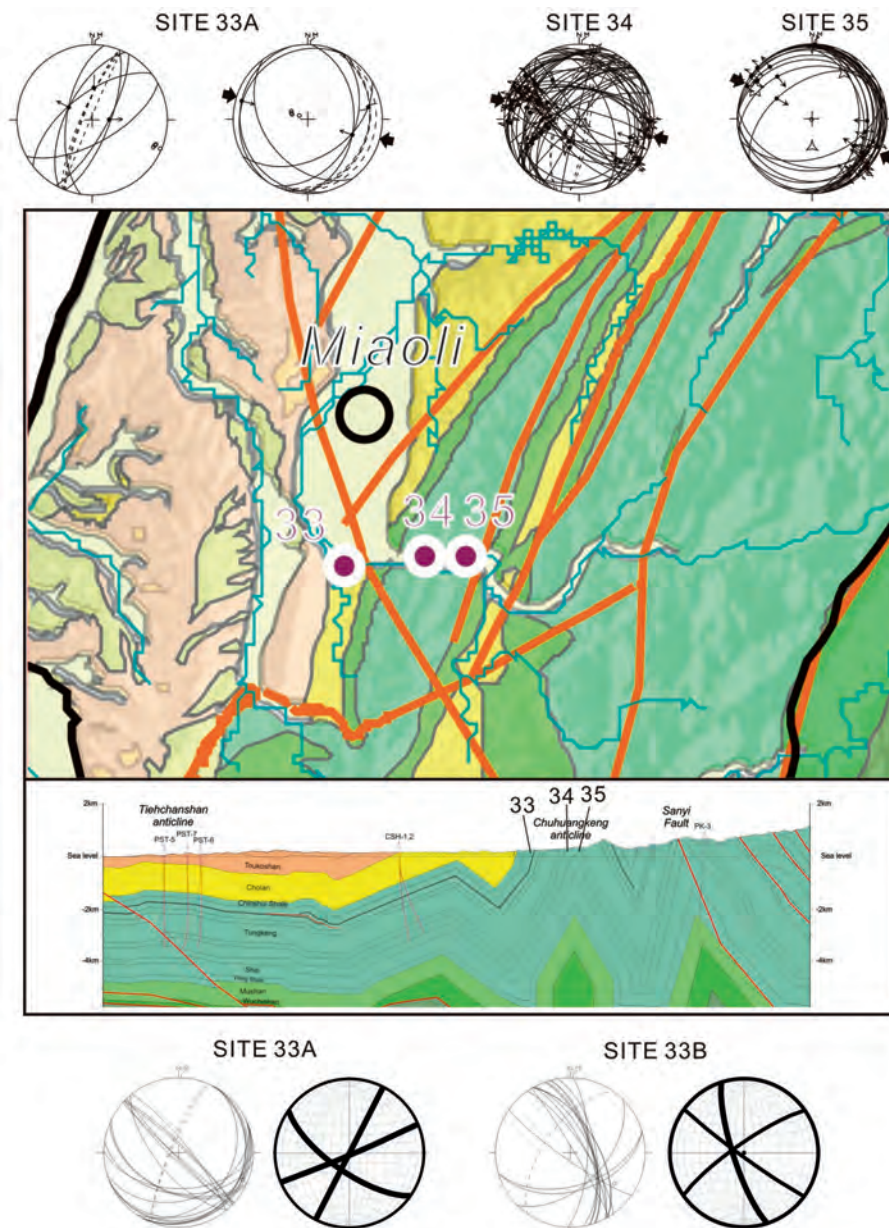


FIG. 6. – Analysis of fracture sets in the Miaoli area of the sub-region III. We present three sites in the foothills. Site 33 (including 33A and 33B) is located in the western limb of the Chuhuangkeng anticline, within the late Miocene Kueichulin Fm. Three sets of bed-perpendicular joint were observed (J1, J3 and J4). See detailed descriptions and analyses in the text. Symbols used for fault-slip and joint sets diagrams are the same as in figure 2. The geological profile crosses in the middle of the sub-region. The color code for geological rock units is the same as in figure 1.

The sites 28 and 28B are located in the footwall near the Paling fault duplex system within the Oligocene Tsuku Fm. Four bed-perpendicular fracture sets were observed. The J1 joints with plumose structure are the most predominant fracture set with orientations of N125°-145°. The J2 joint set orientates N170°-195°. The J3 joint set orientates N090°-100° and the J4 set orientates N030°-050°. The four joint sets are all considered to have formed prior to folding. As for the striated micro-faults, the strike-slip faults indicate a N140° compression during late-folding stage. We also observed some conjugate reverse faults that occurred in the early stage of folding.

The sites 29 and 30 are located at an anticline in the middle of the eastern Hsuehshan Range, whose deformation is characterized by a series of folds (see geological cross section in fig. 5). Two predominant sets of bed-perpendicular joints, which we tend to interpret as J2 and J3 sets, were observed at sites 29 and 29B, with orientations of N165°-170° and N085°-105°, respectively. Four bed-perpendicular joints sets (J1-4) were determined at site 30, with orientations of N165°, N000°-025°, N095°, and N065°, respectively. Strike-slip faults slipped (reactivated) on pre-existing joints and bedding-parallel thrusts were observed at two sites, indicating a N135°-140° compression during folding.

The sites 31 and 32 are located in the eastern edge of the Hsuehshan range within the early Oligocene Szeling Fm. Four bed-perpendicular joint sets were observed at these two sites. The J1 joint set with tension cracks is oriented N120°-145°, and the J2 set N000°-010°, J3 set N090°-115° and J4 set N050°-070°. It is worth noting that the J1, J3 and J4 joint sets are often associated with quartz veins, implying an opening character (presumably in a late tectonic phase).

Sub-region III

In the Miaoli area of the sub-region III, we present three sites in the foothills (fig. 6). Site 33 is located in the western limb of the Chuhuangkeng anticline, within the late Miocene Kueichulin Fm. Three sets of bed-perpendicular joint were observed (J1, J3 and J4). The J1 set is oriented N130°-135°, the J3 set N050°-060°, and the J4 set N030°. We also found conjugate reverse faults, which were interpreted to have occurred prior to or in the very early stage of folding, according to their geometric relation with bedding plane. Paleostress analysis of the reverse faults revealed a N100° compression.

The sites 34 and 35 are located near the fold axis of the Chuhuangkeng anticline, within the middle Miocene Peiliao Fm. Based on the geometric relationships between the derived paleostress axes and the tilted bedding, we determined three episodes of faulting during folding: a conjugate set of reverse faults in the early stage of folding, strike-slip faults during folding and a conjugate set of reverse faults in the late stage of folding. All three episodes show the same compression direction of N100°.

Sub-region IV

In the Taichung-Nantou area of the sub-region IV, we present three locations in Foothills (fig. 7). The first location (sites 36A, 36B, 37) is located at gently E-dipping monocline in the hanging wall of the Chelungpu fault, within the Pliocene

Cholan Fm. This is the youngest rock formation surveyed in this paper, with a burial depth of less than 3-4 km. In each site of this location, we can observe two sets of predominant joints, which is quite different from the usual three or four sets observed in the older rock formations mentioned above. As the strikes of the bedding vary significantly, we used the local bedding strike at each site as the reference for defining the joint sets. We thus determined three sets of bed-perpendicular joints: J4 (N000°) and J2 (N135°-140°) for site 36A; J4 (N040°) and J2 (N005°) for 36B; J4 (N170°) and J1 (N080°) for site 37. No striated micro-faults were measured in this location. It is worth noting that the orientation of the four bed-perpendicular joint sets observed in southern two sub-regions (i.e., sub-regions IV and III) exhibits seemingly a difference of 30°-50° in a counter-clockwise sense compared to that in the northern two sub-regions in NW Taiwan. However, it remains inconclusive because our definition of the fracture sets strongly depends on the regional trend of fold, which clearly shows a curvature in the fold-thrust belt in NW Taiwan as described above.

Site 38 is located within the duplex of the Shangtung fault in the late Miocene Kueichulin Fm. We found 2 sets of bed-perpendicular joints. Because the local bedding varies rather significantly compared to the regional N-S structural trend, we tend to define the joint set with respect to the local bedding strike. That is, the J1 set is defined as the joint set perpendicular to the bedding strike and the J4 set is sub-parallel to the bedding strike at the site. As a consequence, the J1 set is oriented with a spectrum of N145°-160°. The J4 set orientates N055°-060°. We also measured a single datum of joint in the orientation of N030° and one datum in N095°, which might correspond to J2 and J3, respectively. However, because of lack of data, they remain questionable.

The fourth location consists of three sites (39-41), which are located within strongly folded strata in between two major thrust faults, the Shangtung fault and the Shui-changliu fault (see cross section in fig. 7). The sites are in the middle Miocene Peiliao and Taliao Fms with a nearly vertical bedding plane. At site 39, we found 3 predominant sets of bed-perpendicular joints: J1 set (perpendicular to bedding strike and regional N-S fold axis) in an orientation of N080°-095°, J2 set N140° and J3 set N045°-050°. At site 41, two dominant joint sets were observed: J1 set N080°-090° and J4 set in an orientation of N170°-180°. As for the striated micro-faults, we found three steps of compression with: (i) a conjugate set of reverse faults prior to or within the early folding stage, (ii) a conjugate set of strike-slip faults during folding (according to the relationship between the derived stress axis and tilted bedding plane) and (iii) a conjugate set of reverse faults post or in late folding stage. All the above three steps of faulting show a consistent N110°-115° compression.

DISCUSSION

Deep-seated joint sets formed prior to regional folding/thrusting

As described above, based on their geometric relationships with tilted bedding, the fractures sets can be determined regarding their occurrence as pre-, syn-, and post-tilting/

folding products. Our analyses show that most of the pervasive fracture sets, including tensile and shear joints, are found to be perpendicular to the bedding plane and thus agree well with the criteria for pre-tilting/folding structures, although some tensile joints parallel to local fold axis might also possibly be developed during folding. However this needs further detailed investigations. Our analyses revealed rather a complex pattern of fracture sets in NW Taiwan. It also is worth noting that the study area of NW Taiwan is structurally complex with different deformation intensity between foothills and Hsuehshan Range and significant curvature of main structural trends from north to south. The Plio-Pleistocene mountain building due to plate convergence between the Philippine Sea plate and Eurasia certainly does not make the analyses easier. As a consequence, it has become extremely challenging to determine the fracture sets globally in the whole study area. Nevertheless, the

results of the analysis of bed-perpendicular joint sets in NW Taiwan is consistent with previous observations that penetrative joints usually occur at depths under deep-seated tectonic stress [Engelder and Geiser P., 1980; Engelder, 1982] and often at the very beginning of the regional major tectonic events [Bellahsen *et al.*, 2006; Lacombe *et al.*, 2011]. As stated above (see section *The foothills and the Hsuehshan Range in NW Taiwan*), the study area comprises several parallel thrust sheets (fig. 1c), in the fold-thrust belt of NW Taiwan [Ho, 1982, 1986; Suppe, 1980; Lee *et al.*, 1996; Mouthereau *et al.*, 1999; Lacombe *et al.*, 2003]. We thus tend to interpret the majority of the joint sets as deep-seated fractures, which formed at depth during relatively early tectonic events in the foothills and the Hsuehshan Range.

Four different sets of bed-perpendicular joints were commonly observed, although not all four can be found at

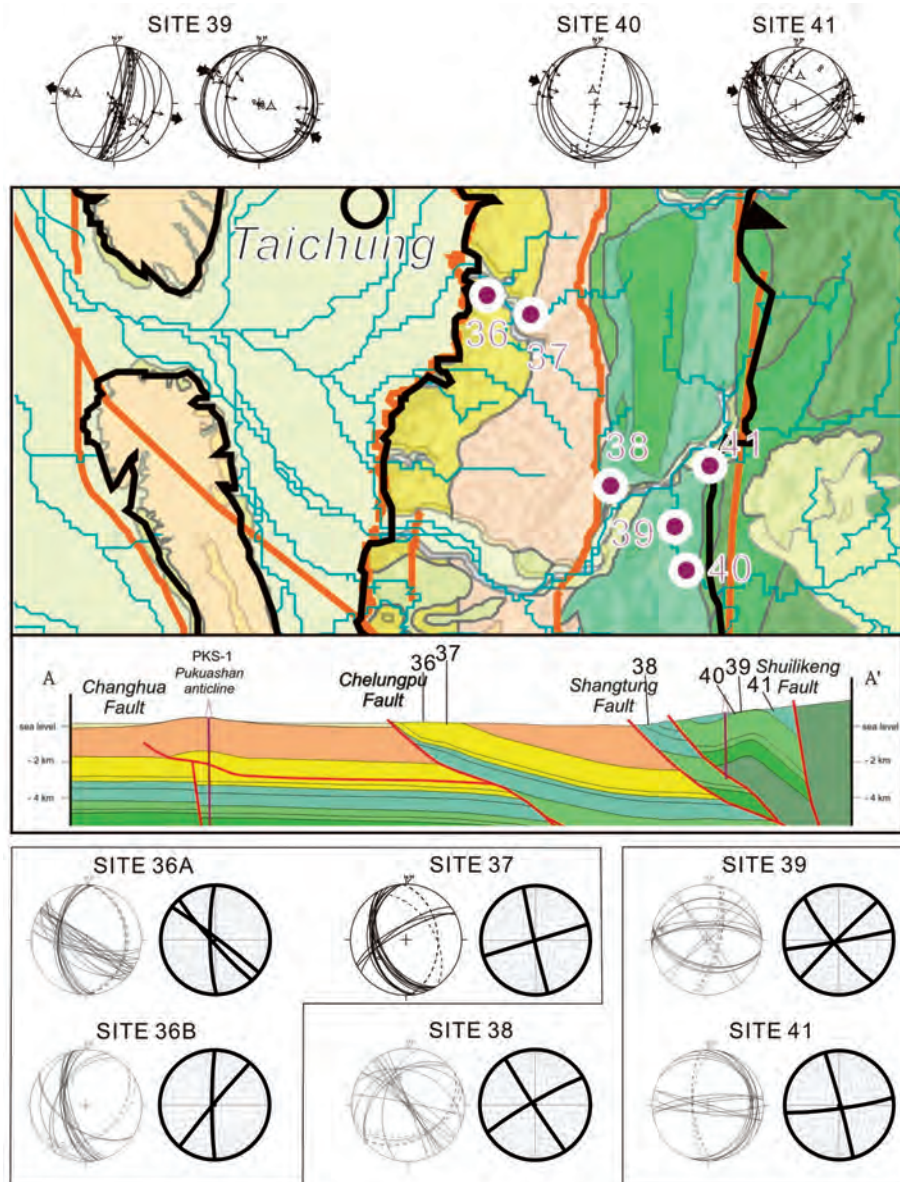


FIG. 7. – Analysis of fracture sets in the Taichung-Nantou area of the sub-region IV. We present two sites (sites 36 and 37) in foothills and four sites (sites 38-41) in the Hsuehshan Range. Symbols used for fault-slip and fracture sets diagrams are the same as in figure 2. The geological profile acrosses the middle of the sub-region. The colors code for geological rock units is the same as in figure 1. See detailed descriptions and analyses in the text.

each site. It appears that two conditions favor the development of multiple sets of joint: (i) occurrence of massive sandstones and (ii) high structural level or high deformation intensity. For instance, the strata with massive sandstones in the Hsuehshan Range often reveal 3-4 joint sets at one site, where the burial depth of the strata is usually around 10 km. The massive sandstones close to major thrusts in the foothills also often show occurrence of a large number of joint sets, which we considered to be caused by high deformation intensity. In contrast, the sites in the foothills show less sets of fractures, typically 2 or 3 joint sets, especially in the younger strata away from the major faults, such as sites 36 and 37 in the Pliocene formations and site 12 in the late Miocene formations.

Conjugate systems of micro-faults and reactivation of pre-existing joints

Regarding striated micro-faults, reverse faults and strike-slip faults are both quite common, although the latter seem to be statistically more abundant. Our field observations indicate that many faults reactivated pre-existing joint planes. For example, the E-W right-lateral strike-slip faults at site 27 (fig. 5) are parallel to the E-W J3 joint set. Many similar orientations of joints and conjugate strike-slip faults in the studied sites suggest that the reactivation of joints as faults is common in the whole area. Moreover, the pitch angle of the strike-slip faults and its relation with the tilted bedding indicate that the strike-slip motion commonly occurred during folding (from early to late folding stages). This is in contrast to the occurrence of 4 joint sets mainly prior to regional folding/thrusting.

In addition to the syn-folding strike-slip striated faults, we also observed syn-folding reverse faults, which are often characterized by a set of bedding-parallel thrusts with or without another conjugate set. The paleostress analysis indicates that the strike-slip faults and reverse faults usually share the same or similar direction(s) of compressive tectonic stress(es), even when two major successive events exist. As a result, the paleostress regime during the development of regional folding/thrusting was likely a transpressional stress regime with a NW-directed average compression (σ_1) and with principal stresses σ_2 and σ_3 of nearly similar values, allowing the corresponding axes to switch from horizontal in the NE direction to vertical. Our results (table II) show that NW-directed compressive tectonics dominated faulting events in both the foothills and the Hsuehshan Range. Furthermore, the greater percentage of strike-slip faults in the Eo-Oligocene Hsuehshan Range compared with the younger Mio-Pliocene foothills probably reflects differences in structural level during deformation in terms of space and time. As the former was buried several kilometers deeper than the latter (fig. 1c), the lower burial of younger formations would significantly reduce the value of the vertical principal stress (i.e., the lithostatic pressure). Thus the value of σ_3 (the minimum stress axis) would approach that of σ_2 (the intermediate stress axis) which enhances the possibility of changing from strike-slip faulting to thrust faulting.

Joint sets in response to regional tectonic stress

As mentioned above, we observed four sets of bed-perpendicular joints in the fold-thrust belt (including foothills and

Hsuehshan Range) of NW Taiwan. In this study we used fold trend as a key-reference to define the fracture sets. For instance, the J4 set is defined as one which is parallel to the regional (or local) fold axis, and J1 is perpendicular to this axis. Indeed, some outcrop observations, especially abutting relationships among the different fracture sets locally provided good constraint and allowed reconstruction of the chronological order of the joint sets. However, these observations are unfortunately sparse. Other observations such as deformation modes (i.e., tensile or shear joints) also could provide valuable information and help to reconstruct evolution of different joint sets. Based on our analyses, we found that the J1 set is usually a set of tensile joints and shear joints often corresponding to J3 or/and J2 sets. But again, sparse observations made the systematic reconstruction difficult, if not impossible, at the present stage. As a consequence, the universal use of the joint sets for the whole study area in NW Taiwan still awaits testing in a more vigorous manner, although comparisons with nearby sites could provide additional constraint to some extent.

Bearing this concern in mind, we nevertheless tried to elucidate the formation of systematic fracture sets in response to the regional tectonic stress. In this regard, previous studies mostly concentrated on a single fold structure [e.g., Bergbauer and Pollard, 2004; Bellahsen *et al.*, 2006] or on a relatively simple multiple-fold structure [e.g., Lacombe *et al.*, 2011], which usually are able to provide a homogeneous direction for each fracture or joint set in the study area. In the case of the fold-thrust belt in NW Taiwan, despite the lack of homogeneity of the fold axis (and tilted bedding), we are able to observe orthogonal joint sets as a quite common feature at each site, complicated by one or two additional joint set(s), which do not help towards the identification of the primary orthogonal tensile joint sets at the many

TABLE II. – Main results of kinematics analysis of fault slickenside measurements. Column 1: site number; Column 2: azimuths and plunges in degrees of σ_1 ; Column 3: σ_2 ; Column 4: σ_3 ; Column 5: $\Phi = (\sigma_2 - \sigma_3) / (\sigma_1 - \sigma_3)$; Column 6: average angle theoretical shear-actual striae in degrees; Column 7: number of fault-slip data.

Site No.	2		3		4		5	6	7
39	139	59	020	15	282	25	0.193	6.3	12
41	106	01	197	39	013	50	0.231	7.9	24
34	284	07	015	09	155	78	0.124	9.6	31
35	141	58	279	24	018	18	0.012	7.3	37
22	123	06	025	53	217	35	0.001	3.1	8
23	327	07	230	45	064	44	.231	5.2	13
5	307	03	044	66	216	22	0.690	9.4	9
5A	309	29	042	05	142	59	0.277	12.5	12
26	301	22	033	05	135	67	0.120	7.1	15
27	315	13	085	69	221	15	0.063	4.8	31
28	333	01	064	19	239	70	0.261	9.0	16
29	136	10	042	20	252	66	0.132	8.6	21
29A	337	11	084	55	240	32	0.450	1.7	5
30	316	10	053	31	211	56	0.314	6.9	21
31	139	07	042	42	237	46	0.420	7.8	17
32	344	21	226	49	089	31	0.503	9.4	14
14	123	38	306	51	214	01	0.523	10.3	15
14A	342	24	202	59	080	17	0.013	8.5	34

sites. Furthermore, the change in the compression directions of two major events (i.e., first in N110°-120° and second in N150°-160°) in the northern part of NW Taiwan makes the analysis more challenging. As a result, the geometric relation between the fracture sets, including the orthogonal tensile and shear joints, and the regional tectonic stress often remains unclear.

A possible scenario, that needs further investigations, would be to interpret the J1 set as a tensile set sub-parallel to the main directions of compression and the perpendicular J4 set as a secondary tensile set parallel to the fold axes. The other sets, J2 and J3, possibly correspond to conjugate shear joints consistent with the direction of main compression (being similar to the direction of J1). Indeed, this is the case, for example in some sites of the Sub-region I with the J1 set oriented N130° to 160° (i.e., direction of σ_1), the J4 set perpendicular (i.e., parallel to the bedding strike) and J2 and J3 sets as conjugate shear joint sets, respectively sinistral and dextral, consistent also with a NW-SE direction of σ_1 . In the Sub-region II, despite the dispersion of the J1 trends, this set corresponds on average to the direction of compression, the J4 set being parallel to the fold axes and only one of the shear sets (J2) being well marked. In the same manner in the sub-region III, the J1 set trending N130°-135° and the J4 set trending N030° are very probably tensile joints since they are respectively perpendicular and parallel to the folds. This scenario, however, is inconsistent with some local observations where J1 is not a tensile but a shear set (see for ex. site 21 in fig. 2 or site 23 in fig. 5) and the reality is probably more complex. Because (i) it is not always easy to distinguish, in the field, an original shear joint from a previous tensile joint slightly reactivated in shear, and (ii) it is common that one of the two sets of a likely conjugate system is missing, which may affect the identification of the existent set as a shear one. Another scenario could be to consider the four joint sets as original tensile sets, the shear behavior being due, in this case, to slight changes in the direction of σ_1 during the jointing process. This may explain the scattered directions of some joint sets as well as the occurrence of both tensile and shear modes in such scattered sets. Only further investigation, especially analysis of pavements, could help to decipher the complex history of jointing in this area and to provide a more robust scenario.

CONCLUSIONS

Based on an analysis of the orientation of about 2500 fractures, including tensile and shear joints, veins and striated

micro-faults, measured in the fold-and-thrust belt of NW Taiwan, and by comparison with the tilted bedding planes and the regional/local folds, we are able to recognize four different sets of bed-perpendicular fractures, which are interpreted to have occurred prior to regional folding/thrusting as deep-seated tectonic joint sets.

Striated micro-faults have been commonly found as both reverse faults and strike-slip faults at many sites. Most of the strike-slip faults used the pre-existing joint sets as slip planes. Many of the reverse faults used the bedding planes as slip planes (bedding-parallel thrusts). In addition, based on their geometric relation with tilted bedding both strike-slip and reverse faults occurred mostly during regional folding/thrusting and can be identified as early-, during and late-folding stages. The paleostress analysis also yielded directions of compression generally consistent with regional folding/thrusting, i.e., perpendicular to the fold axis.

Further, the maximum compressive axis σ_1 derived from the measured fault-slip data in the northern part of the studied area (i.e., sub-regions I and II) showed two major tectonic events: the older one, a N110°-120°, and the younger, a N150°-160° compressive event. This result is consistent with the conclusions of Lacombe *et al.* [2003] who suggested that the evolution of the trend of the maximum compressive stress from N 120° to N 150° in the northern part of the arc, and thus the divergence between compression and regional transport trends, corresponds to a right-lateral wrench deformation parallel to the N070° trending structures of the margin.

The four bed-perpendicular joint sets were formed during the pre-folding stage within several thrust sheets at relatively deep levels. The deformation stage was seemingly a deep-seated regional tectonic event at the very beginning of mountain building in NW Taiwan. This conclusion is further supported by the common observation of the reactivation of pre-existing joints as late-stage faults.

Acknowledgements. – This paper is written in memory of Prof. Jacques Angelier who spent nearly 30 years advising geodynamic research in Taiwan. An exceptionally versatile geoscientist who not only excelled in field studies, but also developed computational programs to evaluate and quantify field data in order to decipher complicated rock formations. Tireless and inspirational, he was a great teacher. Driven by enthusiasm, he routinely ignited the fire of learning in his students. We all remember his teaching fondly and treasure his legacy. The present paper is based largely on field work and discussions carried out with him. We would like to thank O. Lacombe, N. Bellahsen and S. Tavani for their suggestions and their thorough and very constructive comments on this manuscript. This work was supported by the Central Geological Survey; the Institute of Earth Sciences, Academia Sinica; and grants from the National Science Council, Taiwan (NSC101-2116-M-001-005). We also acknowledge the BFT (Bureau Français de Taipei) and the BRT (Bureau de Représentation de Taipei en France) for their constant help.

AHMADHADI F., DANIEL J.M., AZIZADEH M. & LACOMBE O. (2008). – Evidence for pre-folding vein development in the Oligo-Miocene Asmari Formation in the Central Zagros fold belt, Iran. – *Tectonics*, **27**, TC1016, doi: 10.1029/2006TC001978.

ANGELIER J. (1975). – Sur l'analyse des mesures recueillies dans des sites faillés: l'utilité d'une confrontation entre les méthodes dynamiques et cinématiques. – *C.R. Acad. Sci.*, D, **281**, 1805-1808.

ANGELIER J. (1979a). – Néotectonique de l'arc égéen. – Thèse Doct. Etat ès-Science. – *Soc. Géol. Nord, publication spéciale*, **3**, 418 p.

ANGELIER J. (1979b). – Determination of mean principal stress for a given fault population. – *Tectonophysics*, **56**, 17-26.

ANGELIER J. (1984). – Tectonic analysis of fault slip data sets. – *J. Geophys. Res.*, **89**, B7, 5835-5848.

ANGELIER J. (1990). – Inversion of field data in fault tectonics to obtain the regional stress III. A new rapid direct inversion method by analytical means. – *Geophys. J. Internat.*, **103**, 363-376.

References

- ANGELIER J. & MECHLER P. (1977). – Sur une méthode graphique de recherche des contraintes principales également utilisable en tectonique et en séismotectonique: la méthode des dièdres droits. – *Bull. Soc. géol. Fr.*, **7**, **XIX**, 6, 1309-1318.
- ANGELIER J., COLLETTA B. & ANDERSON E. (1985). – Neogene paleostress changes in the Basin and Range – a case study at Hoover dam, Nevada-Arizona. – *Geol. Soc. Amer. Bull.*, **96**, 3, 347-361.
- ANGELIER J., BERGERAT F. & CHU H.T. (1986). – Plate collision and paleostress trajectories in a fold-thrust belt: the foothills of Taiwan. – *Tectonophysics*, **125**, 161-178.
- ANGELIER J., BERGERAT F., CHU H.T. & LEE T.Q. (1990). – Tectonic analysis and the evolution of a curved collision belt: The Hsuehshan range, northern Taiwan. – *Tectonophysics*, **183**, 77-96.
- ARMJO R. & CISTERNAS A. (1978). – Un problème inverse en microtectonique cassante. – *C. R. Acad. Sci.*, Paris, **287**, D, 595-598.
- BARRIER E. (1985). – Tectonique d'une chaîne de collision active: Taiwan. – Thèse Doctorat d'Etat ès-Sciences, *Mém. Sc. Terre Univ. P. & M. Curie*, Paris⁰**85-29**, 492 p.
- BARRIER E. & ANGELIER J. (1986). – Active collision in eastern Taiwan: the Coastal range. – *Tectonophysics*, **125**, 39-72.
- BARRIER E., ANGELIER J., CHU H.T. & TENG L.S. (1982). – Tectonic analysis of compressional structure in an active collision zone: the deformation of the Pinanshan Conglomerates, eastern Taiwan. – *Proc. Geol. Soc. China*, **25**, 123-138.
- BEAUDOIN N., LEPRÊTRE R., BELLAHSEN N., LACOMBE O., AMROUCH K., CALLOT J.-P., EMMANUEL L. & DANIEL J.-M. (2012). – Structural and microstructural evolution of the Rattlesnake Mountain anticline (Wyoming, USA): New insights into the Sevier and Laramide orogenic stress build-up in the Bighorn basin. – *Tectonophysics*, **576-577**, 20-45, doi: 10.1016/j.tecto.2012.03.036.
- BELLAHSEN N., FIORE P. & POLLARD D.D. (2006). – The role of fractures in the structural interpretation of Sheep Mountain anticline, Wyoming. – *J. Struct. Geol.*, **28**, 850-867., doi: 10.1016/j.jsg.2006.01.013.
- BERGBAUER S. & POLLARD D.D. (2004). – A new conceptual fold–fracture model including prefolding joints, based on field data from the Emigrant Gap anticline, Wyoming. – *Geol. Soc. Amer. Bull.*, **116**, 294-307, doi: 10.1130/B25225.1.
- BERGERAT F. (1985). – Déformations cassantes et champs de contrainte tertiaires dans la plate-forme européenne. – Thèse Doctorat d'Etat ès-Sciences, *Mém. Sc. Terre Univ. P. & M. Curie*, Paris, **85-07**, 315 p.
- BERGERAT F. (1987). – Stress fields in the European platform at the time of Africa-Eurasia collision. – *Tectonics*, **6**, 2, 99-132.
- BERGERAT F., ANGELIER J. & BOUROZ C. (1991). – L'analyse des diaclases dans le plateau du Colorado (U.S.A.): une clé pour la reconstruction des paléo-contraintes. – *C. R. Acad. Sci.*, Paris, **312**, sér.II, 309-316.
- BERGERAT F., BOUROZ-WEIL C. & ANGELIER J. (1992). – Paleostresses inferred from macrofractures, Colorado plateau, western USA. – *Tectonophysics*, **206**, 219-243.
- BOUROZ C., ANGELIER J. & BERGERAT F. (1989). – De la distribution des diaclases dans des flexures à la chronologie tectonique: exemples dans le plateau du Colorado (Utah-Arizona, U.S.A.). – *Geodin. Acta*, **3**, 4, 305-318.
- CAREY E. & BRUNIER B. (1974). – Analyse théorique et numérique d'un modèle mécanique élémentaire appliqué à l'étude d'une population de failles. – *C.R. Acad. Sci.*, D, **279**, 891-894.
- CASINI G., GILLESPIE P.A., VERGES J., ROMAIRE I., FERNANDEZ N., CASCIELLO E., SAURA E., MEHL C., HOMKE S., EMBRY J.-C., AGHAJARI L. & HUNT D.W. (2011). – Sub-seismic fractures in foreland fold and thrust belts: insight from the Lurestan Province, Zagros mountains, Iran. – *Petrol. Geosci.*, **17**, 3, 263-282.
- CÉLÉRIER B., ETCHECOPAR A., BERGERAT F., VERGELY P., ARTHAUD F. & LAURENT PH. (2012). – Inferring stress from faulting: from early concepts to inverse methods. – *Tectonophysics*, Special issue "Crustal stresses, fractures, and fault zones: the legacy of Jacques Angelier", doi: 10.1016/j.tecto.2012.02.009.
- CHANG L. S. & CHI W.R. (1983). – Neogene nannoplankton biostratigraphy in Taiwan and the tectonic implications. – *Petrol. Geol. Taiwan*, **19**, 93-141.
- CHI W.R. (1981). – Calcareous nannoplankton biostratigraphic correlation of the Mesozoic and Cenozoic sequences in central, southern and eastern Taiwan, Republic of China. – *Tenth annual Convention*, Indonesia Petroleum Ass., Jakarta, Indonesia, May 26-27, 1-49.
- CHEN C.H., CHU H.T., LIOU J.G. & ERNST W.G. (1983). – Explanatory notes for the metamorphic facies map of Taiwan. – *Spec. Publ. Cent. Geol. Surv.*, China, **2**, 1-32.
- CHU H.T. (1990). – Néotectonique cassante et collision Plio-Quaternaire à Taiwan. – Thèse de doctorat, *Mém. Sci. Terre Univ. P. & M. Curie*, Paris, **90-28**, 292 p.
- COSGROVE J. W. & ENGELDER T. (Eds) (2004). – The initiation, propagation, and arrest of joints and other fractures. – *Geol. Soc., London, Spec. Publ.*, **231**, 330 p.
- ENGELDER T. (1982). – Is there a genetic relationship between selected regional joints and contemporary stress within the lithosphere of North America? – *Tectonics*, **1**, 161-177.
- ENGELDER T. & GEISER P. (1980). – On the use of regional joint sets as trajectories of paleostress fields during the development of the Appalachian plateau, New York. – *J. Geophys. Res.*, **85**, 6319-6341.
- ENGELDER T. & GROSS M.R. (1993). – Curving joints and the lithospheric stress field in eastern North America. – *Geology*, **21**, 817-820.
- ENGELDER T. & PEACOCK D.C.P. (2001). – Joint development normal to regional compression during flexural-flow folding: the Lilstock buttress anticline, Somerset, England. – *J. Struct. Geol.*, **23**, 259-277.
- ETCHECOPAR A., VASSEUR G. & DAIGNIERES M. (1981). – An inverse problem in microtectonics for the determination of stress tensors from fault striation analysis. – *J. Struct. Geol.*, **3**, 51-65.
- GUDMUNDSSON Á. (2011). – Rock fractures in geological processes. – Cambridge University Press, 569 p.
- HANCOCK P.C. (1985). – Brittle microtectonics: principles and practice. – *J. Struct. Geol.*, **7**, 3/4, 437-457.
- HANCOCK P.L. (1986). – Joint spectra. In: R.W. NESBITT & I. NICOL, Eds, *Geology in the real world*. The Kingsley Dunham volume. – Institution of Mining and Metallurgy, London, 155-164.
- HELGESON D.E. & AYDIN A. (1991). – Characteristics of joint propagation across layer interfaces in sedimentary rocks. – *J. Struct. Geol.*, **13**, 8, 897-911.
- HIPPOLYTE J.-C., BERGERAT F., GORDON M., BELLIER O. & ESPURT N. (2012). – Keys and pitfalls in mesoscale fault analysis and paleostress reconstructions, the use of the Angelier's methods. – *Tectonophysics*, Sp. Issue "Crustal stresses, fractures, and fault zones: the legacy of Jacques Angelier", doi: 10.1016/j.tecto.2012.01.012.
- HO C.S. (1982). – Tectonic evolution of Taiwan. Explanatory text of the tectonic map of Taiwan. – Ministry of Economic Affairs, Taipei, 126 p.
- HO C.S. (1986). – An introduction to the geology of Taiwan. Explanatory text of the geological map of Taiwan. – Cent. Geol. Surv., MOEA Taiwan, 2nd ed., 192 p.
- HODGSON R.A. (1961a). – Regional study of jointing in Comb ridge – Navajo mountain area. Arizona and Utah. – *Am. Ass. Petrol. Geol. Bull.*, **45**, 11-38.
- HODGSON R.A. (1961b). – Classification of structures on joint surface. – *Amer. J. Sci.*, **259**, 493-502.
- HSU Y. J., YU S.B., SIMONS M., KUO L.C. & CHEN H.Y. (2009). – Interseismic crustal deformation in the Taiwan plate boundary zone revealed by GPS observations, seismicity, and earthquake focal mechanisms. – *Tectonophysics*, **479**, 4-18.
- HUCHON P., BARRIER E., DE BRAEMACKER J.C. & ANGELIER J. (1986). – Collision and stress trajectories in Taiwan: a finite element model. – *Tectonophysics*, **125**, 179-191.
- LACOMBE O. (2012). – Do fault slip data inversions actually yield 'paleostresses' that can be compared with contemporary stresses? A critical discussion. – *C.R. Geoscience*, **344**, 159-173, doi: 10.1016/j.crte.2012.01.006.
- LACOMBE O., MOUTHEREAU F., ANGELIER J., CHU H.T. & LEE J.C. (2003). – Frontal belt curvature and oblique ramp development at an obliquely collided irregular margin: geometry and kinematics of the NW Taiwan fold-thrust belt. – *Tectonics*, **22**, 3, 1025, 10.1029/2002TC001436.

- LACOMBE O., BELLAHSEN N. & MOUTHEREAU F. (2011). – Fracture patterns in the Zagros simply folded belt (Fars): New constraints on early collisional tectonic history and role of basement faults. – *Geol. Mag.*, **148**, 940-963, doi: 10.1017/S001675681100029X.
- LEE J.C., LU C.Y., CHU H.T., DELCAILLAU B., ANGELIER J. & DEFFONTAINES B. (1996). – Active deformation and paleostress analysis in the Pakua anticline area, western Taiwan. – *TAO*, **7**, 4, 431-446.
- LEE J.C., ANGELIER J. & CHU H.T. (1997). – Polyphase history and kinematics of complex major fault zone in the Taiwan mountain belt: the Lishan fault, northern Taiwan. – *Tectonophysics*, **274**, 97-116.
- LU C.Y., ANGELIER J., CHU H.T. & LEE J.C. (1995). – Contractional, transcurrent rotational and extensional tectonics in northern Taiwan. – *Tectonophysics*, **246**, 129-146.
- MARSHAK S., GEISER P.A., ALVAREZ W. & ENGELDER T. (1982). – Mesoscopic fault array of the northern Umbrian Apennine fold belt, Italy: Geometry of conjugate shear by pressure-solution slip. – *Geol. Soc. Amer. Bull.*, **93**, 1013-1022, doi: 10.1130/0016-7606.
- MARSHAK S. & ENGELDER T. (1985). – Development of cleavage in limestones of a fold-thrust belt in eastern New York. – *J. Struct. Geol.*, **7**, 345-359, doi: 10.1016/0191-8141(85)90040-9.
- MERCIER J.L. & CAREY-GAIHARDIS E. (1976). – La néotectonique plio-quaternaire de l'arc égéen externe et de la mer Égée et ses relations avec la séismicité. – *Bull. Soc. géol. de Fr.*, **7**, **XVIII**, 2, 355-372.
- MOUTHEREAU F. & LACOMBE O. (2006). – Inversion of the Paleogene Chinese continental margin and thick-skinned deformation in the western foreland of Taiwan. – *J. Struct. Geol.*, **28**, 1977-1993, doi: 10.1016/j.jsg.2006.08.007.
- MOUTHEREAU F., LACOMBE O., DEFFONTAINES B., ANGELIER J., CHU H.T. & LEE J.C. (1999). – Quaternary transfer faulting and belt front deformation at Pakuashan (western Taiwan). – *Tectonics*, **18**, 2, 215-230.
- MOUTHEREAU F., DEFFONTAINES B., LACOMBE O. & ANGELIER J. (2002). – Variations along the strike of the Taiwan thrust belt: Basement control on structural style, wedge geometry and kinematics. In: T.B. BYRNE and C.-S. LIU, Eds, *Geology and geophysics of an arc-continent collision, Taiwan, Republic of China, Boulder, Colorado*. – *Geol. Soc. Amer. Spec. Pap.*, **358**, chapter 3, 35-58.
- PARKER J.M. (1942). – Regional systematic jointing in slightly deformed sedimentary rocks. – *Geol. Soc. Amer. Bull.*, **53**, 381-408.
- PEACOCK D.C.P. (2001). – The temporal relationship between joints and faults. – *J. Struct. Geol.*, **23**, 329-341.
- POLLARD D.D. & AYDIN A. (1988). – Progress in understanding jointing over the past century. – *Geol. Soc. Amer. Bull.*, **100**, 1181-1204.
- PRICE N.J. & COSGROVE J.W. (1990). – *Analysis of geological structures*. – Cambridge University Press, 501p.
- QUINTÀ A. & TAVANI S. (2012). – The foreland deformation in the southwestern Basque-Cantabrian belt (Spain). – *Tectonophysics*, **576-577**, 4-19, doi: 10.1016/j.tecto.2012.02.015.
- SENO T. (1977). – The instantaneous rotation vector of the Philippine sea plate relative to the Eurasian plate. – *Tectonophysics*, **42**, 209-226.
- SONNETTE L. (2012). – Etude structurale et paléomagnétique de la courbure des systèmes plissés et chevauchants des arcs de Nice, de Castellan et du Nord-Est de Taiwan. – Thèse de l'Université de Nice-Sophia-Antipolis, 352 p.
- SUPPE J. (1980). – A retrodeformable cross section of northern Taiwan. – *Proc. Geol. Soc. China*, **23**, 46-55.
- SUPPE J. (1981). – Mechanics of mountain building and metamorphism in Taiwan. – *Mem. Geol. Soc. China*, **4**, 67-102.
- TAVANI S., STORTI F., FERNÁNDEZ O., MUÑOZ J.A. & SALVINI F. (2006). – 3-D deformation pattern analysis and evolution of the Añisclo anticline, southern Pyrenees. – *J. Struct. Geol.*, **28**, 695-712, doi: 10.1016/j.jsg.2006.01.009.
- TAVANI S., STORTI F., SALVINI F. & TOSCANO C. (2008). – Stratigraphic versus structural control on the deformation pattern associated with the evolution of the Mt. Catria anticline, Italy. – *J. Struct. Geol.*, **30**, 664-681, doi: 10.1016/j.jsg.2008.01.011.
- TAVANI S., MENCOS J., BAUSÀ J. & MUÑOZ J.A. (2011). – The fracture pattern of the Sant Corneli Bóixols oblique inversion anticline (Spanish Pyrenees). – *J. Struct. Geol.*, **33**, 1662-1680, doi: 10.1016/j.jsg.2011.08.007.
- TENG L.S., CHEN C.H., WANG W.S., LIU T.K., JUNG W.S. & CHEN J.C. (1992). – Plate kinematic model for Late Cenozoic arc magmatism in northern Taiwan. – *J. Geol. Soc. China*, **35**, 1-18.
- TURNER J.P. & HANCOCK P.L. (1990). – Relationships between thrusting and joint systems in the Jaca thrust-up basin, Spanish Pyrenees. – *J. Struct. Geol.*, **12**, 2, 217-226.
- YANG K.M., WU J.C., WICKHAM J.S., TING H.H., WANG J.B. & CHI W.R. (1996). – Transverse structures in Hsinchu and Miaoli area: Structural mode and evolution in Foothills belt, northern Taiwan. – *Pet. Geol. Taiwan*, **30**, 111-150.
- YU S.B., CHEN H.Y. & KUO L.C. (1997). – Velocity field of GPS stations in the Taiwan area. – *Tectonophysics*, **274**, 41-59.